Scanning tunneling microscope for magneto-optical imaging

M. W. J. Prins,[a] R. H. M. Groeneveld, D. L. Abraham,[b] R. Schad, and H. van Kempen
Research Institute for Materials, University of Nijmegen, Toernooiveld 1, 6525 ED Nijmegen, The Netherlands

H. W. van Kesteren
Philips Research Laboratories, Prof. Holstlaan 4, 5656 AA Eindhoven, The Netherlands

(Received 24 July 1995; accepted 2 January 1996)

Images of magnetic bits written in a Pt/Co multilayer are presented. Using photosensitive semiconducting tips in a scanning tunneling microscope the surface topography as well as the polarization-dependent optical transmission are measured. Magnetic contrast is achieved by detection of the Faraday effect. Magneto-optical lateral resolution of 250 nm is demonstrated.

I. INTRODUCTION

Magnetic imaging is an important issue in both fundamental science and modern technology. Further development of magnetic data-storage technology requires magnetic imaging with a resolution of at least the size of the magnetic structures. As the bit size in magnetic recording goes beyond the optical diffraction limit, the classical far-field imaging techniques such as Kerr microscopy have reached their limits. Other approaches have been further improved or have recently emerged, which are derivatives of electron microscopy and scanning probe microscopy. To the former belong the Lorentz force microscopy and the scanning electron microscope with spin polarization analysis (SEMPA), both requiring a complicated experimental setup under vacuum conditions. Among the scanning probe techniques the magnetic force microscope (MFM) is the most commonly employed type, having a high resolution in a relatively simple setup. A problem is the contrast mechanism itself, which may lead to alterations in the domain structure of the sample due to the interaction with the magnetic tip. Additionally, it is sensitive only to gradients in the magnetic field, so that this method images the domain walls rather than giving information about the magnetization inside the domains.

These drawbacks can be overcome by a scanning probe microscope, which is based on the interaction of polarized light with the magnetic sample. Unlike the conventional Kerr microscope, it is working in the optical near-field regime resulting in much higher resolution. This is achieved by either illuminating or detecting with near-field sources or probes. In the first successful demonstration of this approach the light was guided to the sample through a tapered optical fiber, detecting the change in polarization of the transmitted radiation.[1] This optical fiber technique has still some technical problems such as the loss of intensity in the tapered part of many orders of magnitude, leading to heating problems, or the distance control, which is done by shear force detection that does not necessarily ensure a constant tip-to-sample distance. Recent alternative approaches try to avoid the light transmission through optical fibers, using instead macroscopic illumination of the sample combined with a microscopical local detector. In one of these experiments a small Ag cluster, illuminated close to the surface plasmon resonance frequency, serves as a local, microscopic detector.[2] Another approach uses a local photodetector which is produced on an AFM cantilever.[3] Its ultimate resolution is limited by the size of the structures fabricated on the tip.

A more simple solution, which we demonstrate in this contribution, uses a semiconducting (GaAs) tip which acts as a photodiode due to the electric field generated in the depletion region close to the surface.[4] The photocurrent is detected by keeping the tip within tunneling distance to the sample in a usual scanning tunneling microscope (STM). Accordingly, two types of contrast are obtained simultaneously. First, the STM feedback action reflects the usual topography of the sample surface. Second, using a circularly polarized light source, contrast is achieved by the magnetization dependent attenuation of the light intensity due to the Faraday effect. This way it is possible to image magnetic domains prewritten in a Co/Pt multilayer. The resolution obtained so far is about 250 nm as derived from the steepness of the contrast change at the domain borders. The advantages of the magneto-optical near-field STM are the absence of magnetic tip–sample interaction, the fact that it can operate in an external magnetic field and under ambient conditions, and the submicrometer magnetic resolution. Possibilities of further improvement are discussed.

II. EXPERIMENT

The experiments were performed in a STM at ambient temperature and pressure. As depicted in Fig. 1, a semiconductor tip (T) was illuminated along the tip axis through a semitransparent sample (S). The sample was constituted of a thin ferromagnetic film on a glass substrate. A magnetic-field

[a]Present address: Philips Research Laboratories, Prof. Holstlaan 4, 5656 AA Eindhoven, The Netherlands.
[b]Present address: Knobbe, Martens, Olson, and Bear, 620 Newport Center Drive, Newport Beach, CA 92660.

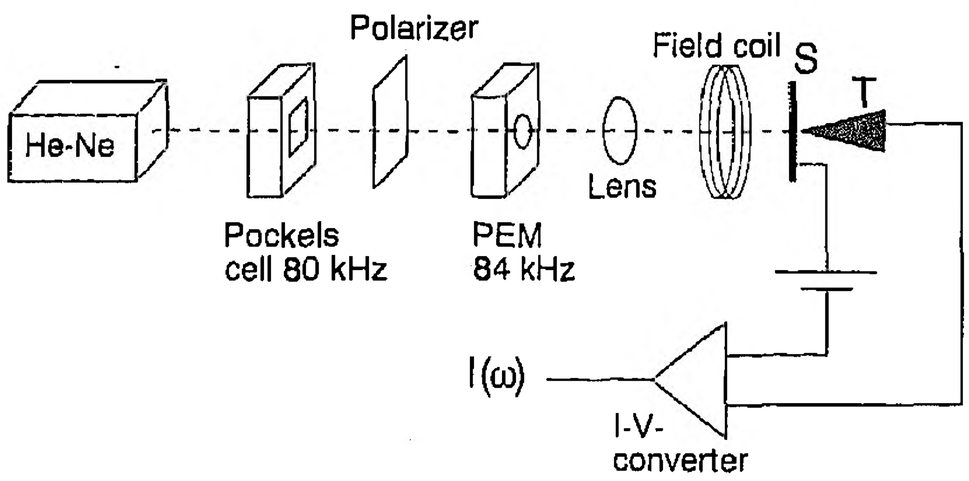

FIG. 1. Experimental arrangement.

coil was placed around the STM, producing dc fields up to 80 kA/m and pulsed fields of 800 kA/m. The optical beam of a linearly polarized single-mode HeNe laser (633 nm) was guided through a Pockels cell and a polarizer, which provided an intensity modulation (IM) of a few percent at 80 kHz. Next the beam passed through a photoelastic modulator (PEM), introducing an 84 kHz sinusoidal polarization modulation (PM) between right- and left-handed circular polarization of the light. Finally the beam was focused onto the tunnel junction by a 30 mm focal length objective, to a spot of 20 ± 5 μm diameter. To the metallic sample an external voltage V_m was applied. The current I was measured by a homemade 100 mV/nA current-to-voltage converter with a bandwidth of about 100 kHz. This signal was fed into two lock-in amplifiers for phase-sensitive detection of the current modulations. The bandwidth of the STM constant-current regulation system was 2 kHz. At every point of the scan the topographical height was recorded simultaneously with the current modulations at 80 and 84 kHz.

The intensity modulation signal served to determine the optical response of the tip R, being the ratio of the detected relative tunnel current modulation $\Delta I^{\mathrm{IM}}/I$ with respect to the preset relative modulation of incident optical power $\Delta P/P$. The calibrated polarization modulation signal is $\Delta I^{\mathrm{PM}}/I$ divided by the response R and multiplied by $\sqrt{2}$ to account for the rms value of sinusoidal modulation. In order to be consistent with the definition of Faraday ellipticity[5] the circular dichroism signal (CD) is the calibrated PM signal divided by a factor of 2.

The GaAs tips were prepared by cleaving (001) wafers along (110) and (1$\bar{1}$0) directions, forming a corner bounded by these planes. The GaAs was p type of 10^{17} cm^{-3} doping density. Inspection by scanning electron microscopy (SEM) and STM showed that cleavage produced well-defined corners with tip apex radii of smaller than 100 nm. The Pt/Co multilayer consists of a 6 Å Pt base layer and 20 pairs of 3.5 Å Co and 6 Å Pt layers evaporated on a glass substrate. The sample exhibits perpendicular magnetic anisotropy and was homogeneously magnetized except for rows of thermomagnetically written bits of opposite magnetization. The bits have a diameter of 0.8 ± 0.2 μm and are spaced 2.0 ± 0.1 μm apart within the rows. The rows are separated by a distance of 2–3 μm.

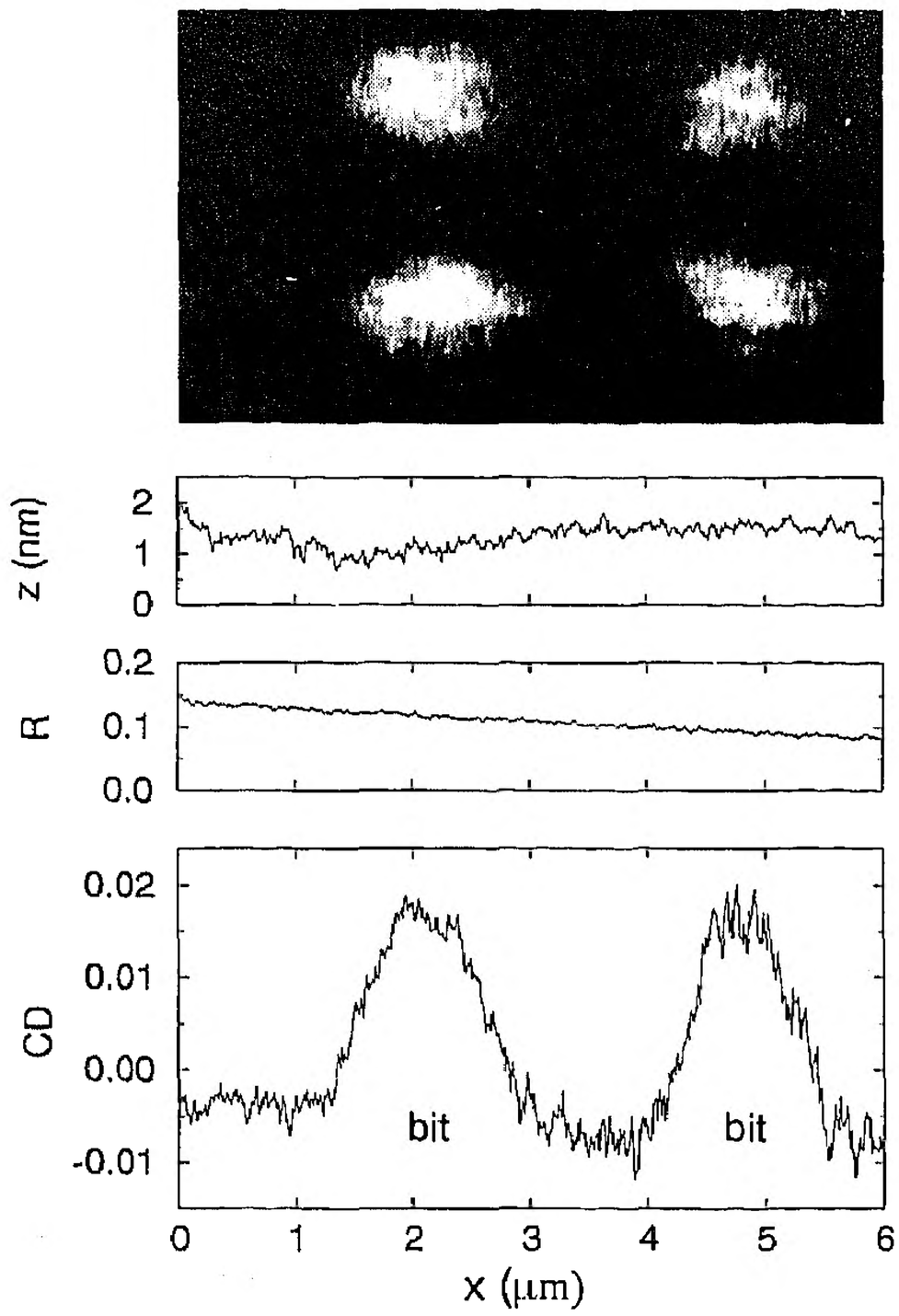

FIG. 2. (A) Circular dichroism (CD) image of magnetic bits prewritten in a Pt/Co multilayer. Curves (B)–(D) represent topography, response, and circular dichroism, respectively, measured on a horizontal line scan over the two topmost bits of image (A). Recorded with a p-type 4×10^{17}-cm^{-3} doped GaAs tip. Incident illumination intensity 1×10^{6} W m^{-2}. Set dc tunnel current I=0.5 nA, reverse applied bias voltage V_m=0.5 V.

III. RESULTS AND DISCUSSION

Figure 2 demonstrates the magneto-optical imaging capabilities of our semiconductor tips. Figure 2(A) shows a 6.0 $\times3.6$ μm^2 image of the magnetic bits, taken in 8 min time. The bits were detected by the CD signal measured while scanning. In this image the bits were written in rows from bottom to top. Indeed, we observe that in this direction the interbit distance is approximately 2 μm. Outside the area with the bits a CD signal with uniform sign has been observed, whereas on the bits a sign reversal of this signal was found. The observation of a sign reversal is in agreement with the fact that the bits have opposite magnetization with respect to the rest of the sample. Further details are given in Figs. 2(B)–2(D), showing the simultaneously measured topography, response R, and CD signal on a line scan over the two topmost bits of Fig. 2(A). The fine structure on the topographic signal is due to the presence of microcrystallites. Note that the scales for the topographic corrugation and the lateral coordinate differ by three orders of magnitude. The response R is essentially flat and merely shows a gradual lateral variation, probably due to differences in light power arriving at the sample. It is only in the CD signal that the bits become clearly visible. The difference of CD within and outside the bits yield a value for the measured magnetic circular

FIG. 3. Circular dichroism image of magnetic bits, including interferencelike features. Area 6.1×3.0 μm^2.

dichroism (MCD) of 1.1%. From the steepest edges observed in our images we estimate the lateral optical resolution of a p-type GaAs tip of 10^{17} cm^{-3} doping density to be 250 nm at the specified operating conditions.

Occasionally, the CD images taken on the sample area with prewritten bits were perturbed by interferencelike features, of which a dramatic example is shown in Fig. 3. The vertical axis represents the slow scanning direction. Neither the simultaneously measured topographical image nor the image of the optical response R revealed any irregularities. In the upper part of the CD image (most clearly in the upper left-hand corner) we observed a horizontal line of discontinuity in the interference rings. Above that line the interference pattern seems to be "dragged" along in the slow scanning direction. At the top of the image the scanning was suddenly interrupted by instabilities in the feedback system, after which the tip did not any more yield proper scans. We observed interferencelike features in several separate measurements, most notably on a part of the sample with a visible density of tiny fragments, deposited by crashing a previous GaAs tip. Furthermore, whenever the scanning tip would approach the center of the rings, the scanning was interrupted by tunneling instabilities. We attribute these observations to the presence of a particle on the sample surface in the vicinity of the imaged area. We believe that the pattern of rings is due to the interference of the normally transmitted light with the waves scattered by the particle. A dragged interference pattern (as at the top of Fig. 3) may then be explained as the result of a weakly bound particle that is slowly moved over the surface by the scanning tip. In this interpretation, the fact that the center of the rings could never be imaged is understandable if the particles are too large to be imaged, if the particles are weakly attached to the sample surface, or if the particles badly conduct the current to the sample surface. A detailed understanding of the shape of the observed interference image requires a model calculation on the near-field optical pattern that is set up between the sample, the tip, and the particle; this issue remains to be investigated.

The optical resolution is given by the active detector size of the tip—represented by the so-called photocarrier collection radius—which is essentially determined by the optical penetration depth, the minority-carrier diffusion length, and the profile of the band-bending region, all of which can be tuned to be of subwavelength extent. The main optical parameter is the penetration depth of the light, which in GaAs is 250 nm for radiation of 633 nm wavelength.[6] Important electrical transport lengths are the minority-carrier diffusion length (~μm)[7] and the depletion region width (~70 nm). A decrease of collection volume may be achieved by

(i) a reduction of the diffusion length (higher doping density, or a different semiconductor material),
(ii) a reduction of the optical penetration depth to below the depletion region width (radiation of shorter wavelength), or
(iii) a reduction of the focusing properties of the depletion field (forward bias operation, or a sharper tip).

A resulting reduction of detectable photocarrier current has to be compensated for by increasing the optical power. Special care will have to be taken to avoid signals due to thermal expansion to start dominating, for example, by increasing the modulation frequencies. As an example, having 10 mW light power absorbed in the tip within a 20-μm-spot diameter and drawing 0.5 nA of tunnel current, we estimate a lateral optical resolution of 6 nm to be achievable with a tip having an optimized collection volume of photocarriers.

An advantage of the above-presented technique is that simultaneously magnetic information as well as high-resolution topographic information is extracted. Furthermore, since the probe is nonmagnetic, one can study the sample properties upon application of an external magnetic field.[8] A measurement scheme that is closely related to the above presented technique is spin-polarized tunneling by optical spin orientation in GaAs. The magneto-optical Kerr/Faraday effect is sensitive to the bulk magnetization, whereas spin-polarized tunneling is sensitive to the spin polarization of electronic states at the sample surface. The respective effects may be separated by their dependence on excitation wavelength, surface preparation, and bias voltage. Ideally, one would like to combine the two measurements, so as to be able to simultaneously measure sample topography, bulk magnetization, and surface spin structure with (sub)nanometer resolution.

ACKNOWLEDGMENTS

The authors are pleased to acknowledge the technical support of A. F. van Etteger, J. Hermsen, and J. Gerritsen. The authors thank A. van Geelen for supplying semiconductor materials. G. J. Bauhuis measured the doping density of our wafers. Part of this work was supported by the Stichting Fundamenteel Onderzoek der Materie (FOM), which is financially supported by the Nederlandse Organisatie voor Wetenschappelijk Onderzoek (NWO). The research of R. H. M. G. has been made possible by a fellowship of the Royal Netherlands Academy of Arts and Sciences (KNAW).

[1]E. Betzig, J. K. Trautman, R. Wolfe, E. M. Gyorgy, P. L. Finn, M. H. Kryder, and C.-H. Chang, Appl. Phys. Lett. **61**, 142 (1992).
[2]T. J. Silva, S. Schultz, and D. Weller, Appl. Phys. Lett. **65**, 658 (1994).
[3]H. U. Danzebrink, O. Ohlsson, and G. Wilkening (unpublished).

[4]M. W. J. Prins, M. C. M. M. van der Wielen, R. Jansen, D. L. Abraham, and H. van Kempen, Appl. Phys. Lett. **64**, 1207 (1994); M. W. J. Prins, R. H. M. Groeneveld, D. L. Abraham, and H. van Kempen, *ibid.* **66**, 1141 (1995); M. W. J. Prins, R. Jansen, R. H. M. Groeneveld, A. P. van Gelder, and H. van Kempen, Phys. Rev. B (in press).

[5]W. Reim and J. Schoenes, in *Ferromagnetic Materials*, edited by K. H. J. Buschow and E. P. Wohlfarth (Elsevier, Amsterdam, 1990), Vol. 5, p. 134.

[6]D. E. Aspnes and A. A. Studna, Phys. Rev. B **27**, 985 (1983).

[7]R. K. Ahrenkiel, in *Minority Carriers in III–V Semiconductors: Physics and Applications*, edited by R. K. Ahrenkiel and M. S. Lundstrom, Semiconductors and Semimetals, Vol. 39 (Academic, San Diego, 1993), Chap. 2, p. 39.

[8]M. W. J. Prins, M. C. M. M. van der Wielen, D. L. Abraham, H. van Kempen, and H. W. van Kesteren, IEEE Trans. Magn. **MAG-30**, 4491 (1994).